Characterization of different Al-to-steel dissimilar welds using an innovative FSW-based process.

Presenting author: Aude Simar*

Norberto Jiménez Mena*, Pascal J. Jacques*, Camille van der Rest*

*Université Catholique de Louvain (UCL), Institute of Mechanics, Materials, and Civil Engineering, IMAP, Place Sainte Barbe 2 bte L5.02.02, B-1348 Louvain-la-Neuve, Belgium

SYNOPSIS

The innovative friction melt bonding process to join dissimilar materials in lap-joint configuration has been applied to weld aluminium to steel in lap-joint configuration. In this process, a flat cylindrical tool is pressed against a top sheet of steel. The frictional heat generated is large enough to be transmitted through the steel to an aluminium sheet placed below and melt it at the interface. This allows controlling the formation of Fe/Al intermetallics that are responsible for the bonding. Several welds at different advancing speeds of the tool have been carried out using Ultra-low-carbon (ULC) and dual-phase (DP) steels and 1050, 2024, 6061 Al alloys. The microstructure was observed and the thickness of the intermetallic was measured as thin as 2-3 µm at higher advancing speeds. Hardness measurements were performed to assess the different affected zones as well as lap-shear tests to measure the strength of the bonding.

INTRODUCTION

Automotive industry has been an active actor in the development of high performance steels. This is the case of the advanced high-strength dual-phase steel (DP). However, the tight legislations to reduce the greenhouse gas emissions, promoted by governmental bodies, have increased the application of lightweight materials, such as aluminium, to improve car efficiency. Cui *et al.* [1] stated that the lightening of the car structures, keeping the crashworthiness properties without cost increase, is achievable by designing multi-material structures, mainly focusing on aluminium and advanced high strength steels. Nevertheless, the joining of these two materials in the automotive body requires innovative processes due to the dissimilar nature of the base materials. Conventional methods such as Gas Tungsten Arc Welding (GTAW) and Resistance Spot Welding are not suitable mainly because of the fast formation of brittle Fe/Al intermetallics that weaken the bonding and the highly different melting temperatures, fostering that only aluminium melts during the welding [2, 3, 4]. These are the reasons why current joining methods in automotive industry involve mechanical clinching, self-piercing riveting and friction stir spot welding [5]. In general, these methods offer a lower resistance than a metallurgical bonding in terms of strength and fatigue, increase of stress concentration and do not provide continuous sealing [6, 7].

However, the formation of an Fe/Al intermetallic is unavoidable, even in solid-state processes as observed by Chen *et al.* [8] for friction stir welding between Al 6061 and AISI 1018. According to Tanaka *et al*. [9], the thickness of the intermetallic compounds strongly influences the fracture strength of the joints, predicting an optimum for thicknesses around 0.5-1.5 um. Sierra *et al.* [10] tested keyhole laser welding on Al-to-steel lap-joint welds obtaining defect-free seams that resisted up to 250 MPa in tensile tests with IML thicknesses down to 5 µm. In their respective works Fan *et al.* [11] and Meco *et al.* [12] controlled the thickness of the IML by changing the power input in overlap conduction laser welding. However, laser equipment remains expensive, limiting the implantation of this technique.

In this framework, an innovative process able to carry out dissimilar lap-joint welds between metals with large differences in melting temperature has been patented by the authors [13, 14]. In this process, a stack with the two materials to be welded is clamped, placing the material with lower melting temperature, Al, under the steel sheet (Figure 1). Subsequently, a non-consumable pinless cylindrical tool is rotated and pressed against the surface of the steel plate, moving at a given advancing speed. Heat is then generated due to the friction between the two surfaces in relative movement and to the severe plastic deformation taking place in the steel below the tool. This heat is transmitted by conduction to the aluminium melt it at the interface and favour the reaction between Al and Fe to form the intermetallic layer (IML) that will be responsible for the bonding once the weld has cooled down.

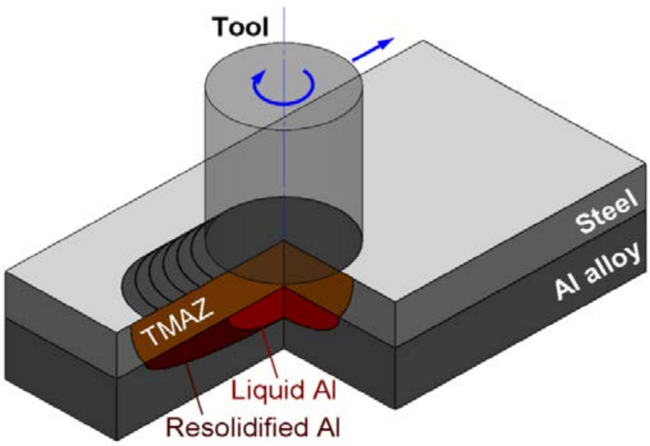

Figure 1: Layout of friction melt bonding process [13]

This new process is attractive due to its simplicity, no need of shielding gas and negligible prior preparation of the sheets. Furthermore, a wide range of advancing speeds up to 700 mm/min can be attained for thin steel sheets with a limited tool wear (particularly for soft steels such as microalloyed steels) and no keyhole at the end of the pass. In addition, the absence of pin and complex geometries of the tool greatly reduces its cost.

EXPERIMENTAL METHODS

Several tests have been carried out using either ULC or DP600 steel grades with 1050, 2024 and 6061 Al alloys. The respective thicknesses and compositions can be found in Tables 1 and 2.

	Weight %									
	C	**Mn**	**Si**	**S**	**P**	**Ti**	**Nb**	**N**	**Cr**	**Mo**
ULC (0.8 mm)	0.013	0.136	0.01	0.005	0.0132	0.002	0.003	<0.008		
DP600 (1.8mm)	0.08	1.51	0.26	0.004	0.02	-	-	-	0.35	0.06

Table 1: Chemical compositions of steel plates

	Weight %								
	Cu	**Fe**	**Mg**	**Si**	**Ti**	**V**	**Cr**	**Zn**	**Mn**
1050 (1 mm)	0.07	0.09	0.85	0.03	0.02	0.01	-	-	-
2024 – T3 (2 mm)	4.40	0.18	1.50	0.10	0.02	-	0.01	0.18	0.51
6061 – T6 (1 mm)	0.24	0.44	0.92	0.56	0.02	0.01	0.19	0.04	0.05

Table 2: Chemical compositions of Al plates

The stack is completed with a backing plate made of steel. The size of the sheets is 250x80 mm and the run of the tool is 220 mm. The first 100 mm are used to heat the tool to the working temperature and the next 120 mm are considered to be in a pseudo-steady-state regime and were used for subsequent analysis.

The chosen tool is a 16 mm radius cylinder made of cemented tungsten carbide with 6%Co. Its rotational speed is kept constant at 2000 rpm while the advancing speeds varied between 100 and 700 mm/min.

RESULTS AND DISCUSSION

SEM and EBSD observations

As a result of the reaction between the molten Al and solid Fe, an intermetallic layer (IML) is formed. The backscattered electron SEM image of Figure 2a shows the microstructure of the cross section at the interface of a DP600-6061 weld. Figure 2b corresponds to the superposition of phase coloured and band contrast EBSD maps for a ULC-1050 weld. It clearly differentiates the two compounds found in the IML; a constant layer of $FeAl_3$ of around 1 µm thickness and very fine grains and a second layer of Fe_2Al_5 with a tongue-like morphology. This is in agreement with what has been reported in previous works on Fe-Al reactivity [9, 15].

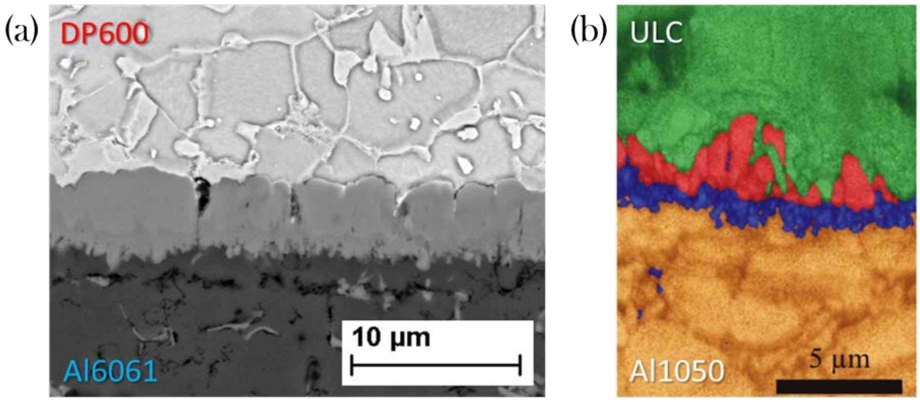

Figure 2: (a) SEM observation of the DP-6061 weld interface and (b) EBSD contrast map of ULC-1050 weld with phase colouring, green for ULC, red for Fe2Al5, blue for FeAl3 and yellow for Al. Figure 2b out of [13].

Naoi and Kajihara [16] determined that the growth of the IML follows a parabolic expression controlled by volume diffusion of Al through Fe_2Al_5. The thickness of the IML depends on time and temperature, and, therefore, on the thermomechanical cycles influenced by the process parameters. In Figure 3, the variation of the thickness of the intermetallic layer as a function of the advancing speed is presented for different steel-aluminium combinations. The faster the tool advances, the shorter the thermomechanical cycle is, resulting in a thinner IML.

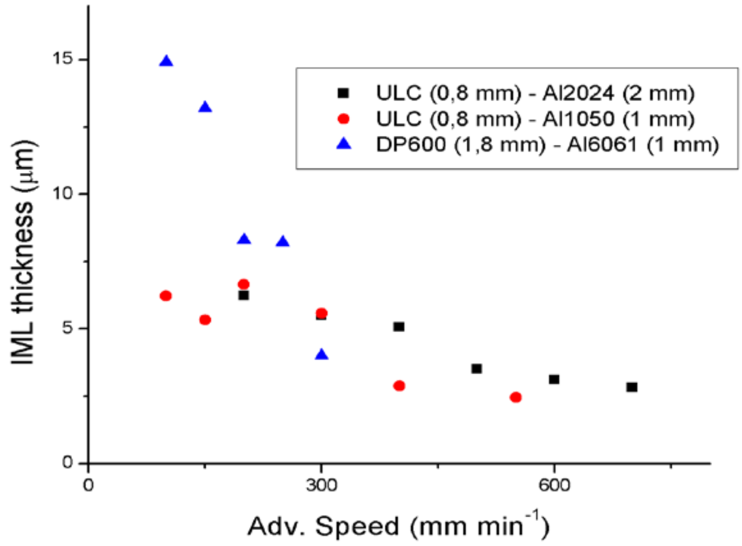

Figure 3: Evolution of the intermetallic thickness as a function of the advancing speed for various aluminium-steel combinations and sheet thicknesses (some data out of [13])

An IML down to 2-3 um is achieved with an advancing speed of 700 mm/min. It is also interesting to point out that the contact properties of the tool-DP and tool-ULC couples are different. A higher heat input is reached when the tool is in contact with DP steel, leading to a thicker IML at lower advancing speeds. A possible explanation for this phenomenon relies on the higher yield strength and work hardening ability at the welding temperatures for DP steel compared to ULC steel. It is also worth noting that the difference in sheet thicknesses significantly affects the temperature field and explains some differences in IML thicknesses.

There is a clear difference in the resulting microstructures of ULC and DP steels. For ULC steel (Figure 4), the thermomechanically affected zone shows a refined grain size as typically observed for Friction Stir Processing of steels [17, 18]. Regarding DP steel (Figure 5) the process temperatures above the ferrite to austenite transus promotes austenization, resulting in a bainitic microstructure after fast cooling in the thermomechanically affected zone.

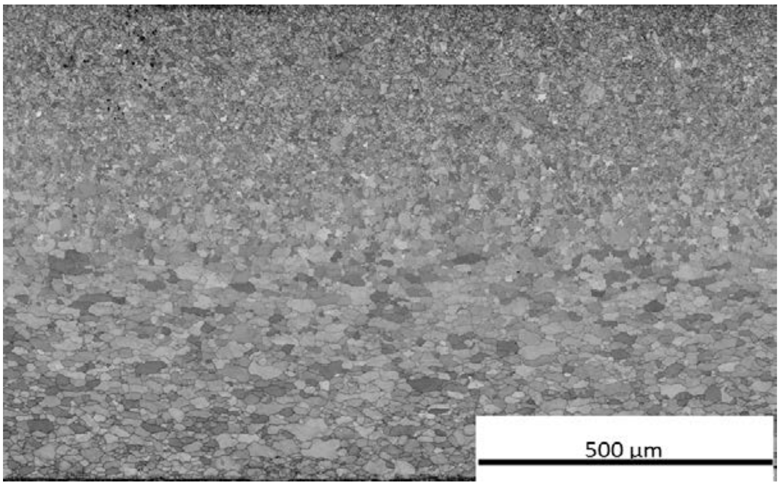

Figure 4: EBSD contrast map showing the refining of the ULC's ferrite grains in the thermomechanically affected zone (top)

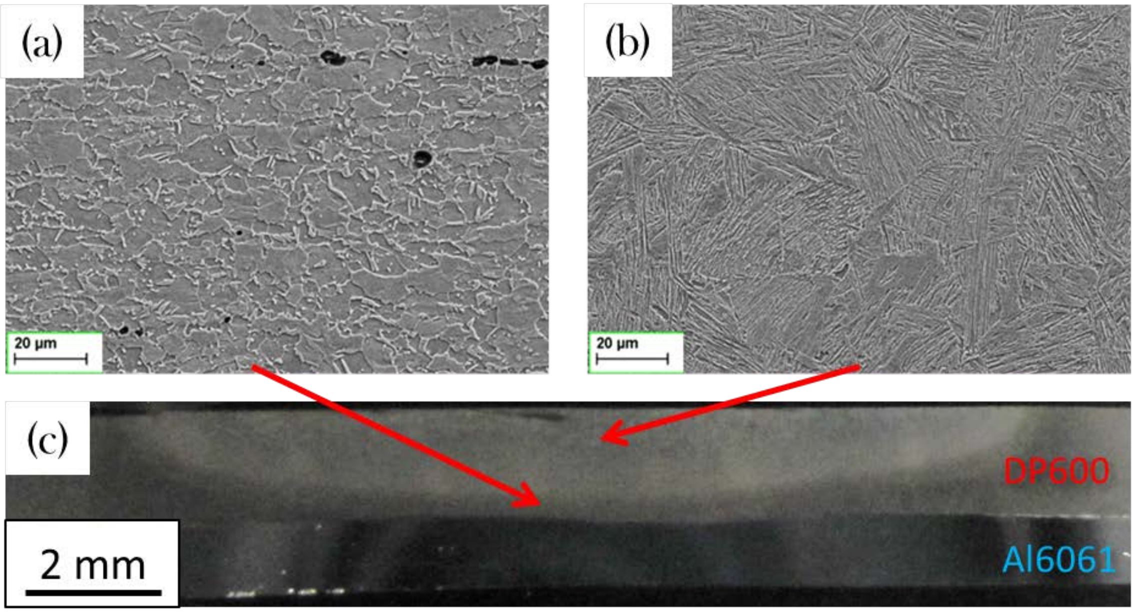

Figure 5: SEM micrograph of the DP steel base material showing a microstructure of martensite islands in a ferrite matrix (a) and the bainitic microstructure as a result of the full austenization and fast cooling in the thermomechanically affected zone (b). Lines indicate the position of the pictures in a cross section after nital etching on steel (c).

Hardness measurements

As a result of the microstructure evolution, a hardness profile was performed on the affected zones of the base materials under the tool on a DP600-6061 weld (Figure 6). The as-received DP steel and 6061-T6 sheets have hardness values equal to 217 and 130 HV1, respectively. The hardness increase on the DP steel is due to the formation of martensite/bainite in the thermomechanically affected zone. The drop of hardness in the aluminium fusion zone is due to precipitate solutionizing and alloying element segregation. The hardness in the heat affected zone of aluminium is also lower than in the base material as the fine β” precipitates in the T6 state are dissolved for the smallest ones and coarsened for the larger ones. [19]

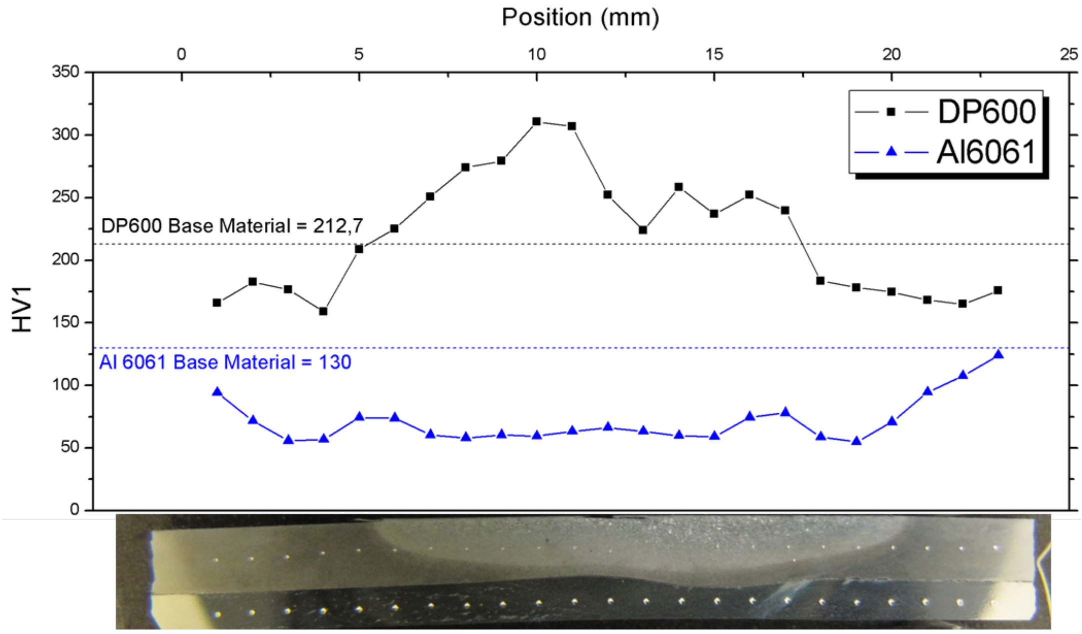

Figure 6: HV1 hardness profiles of DP600 and Al 6061 respectively (top) and macrography of the weld (bottom)

Lap-shear tensile tests

Lap shear tests were performed in ULC - Al1050 and ULC - Al2024 welds. Figure 7 compares the tensile strength as a function of the advancing speed. The results are grouped in three sets depending on the location of the fracture. For the first set, the fracture occurred in the heat affected zone of the 1mm-thick Al base material, showing an UTS mean value of 76 MPa. The second set corresponds to the fracture of the ULC steel base material in the ULC-Al2024 welds, with mean UTS similar to the one of base UCL steel (289-300 MPa). The third set includes the ULC-Al2024 welds with fracture close to the interface due to the larger presence of solidification defects on the aluminium side. The absence of fracture in the IML suggests that, even with an IML thickness larger than a few microns, its fine grain size does not deteriorate the weld strength with respect to the base materials.

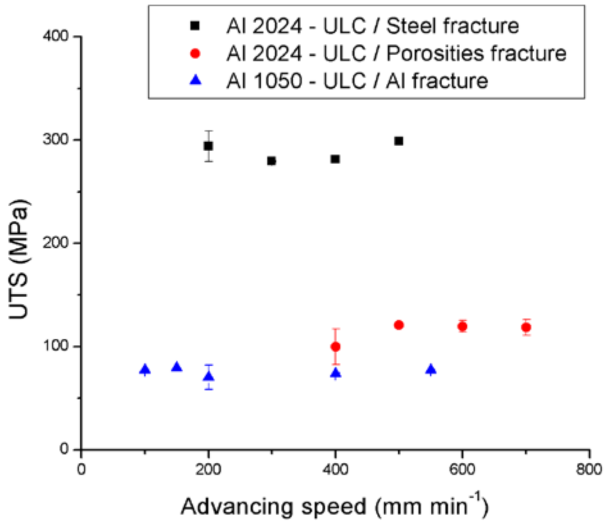

Figure 7: UTS as a function of the advancing speed. The three sets of point correspond with the mode of fracture (some data out of [13])

The presence of porosity as a solidification problem in these welds seems to be related to both process parameters and material composition. Figure 8 shows a comparison of 1050 and 6061 welds at low and high advancing speed. This porosity is significantly reduced at lower advancing speeds. In accordance with Eskin *et al.* [20], the composition also plays a fundamental role in hot tearing during solidification, 6061 alloy being more susceptible than 1050. This explains why such defects are not observed in welds made of 1050 aluminium alloy. For advancing speeds larger than 250 mm/min in DP-6061 welds, the presence of porosity is too significant for sufficient bonding.

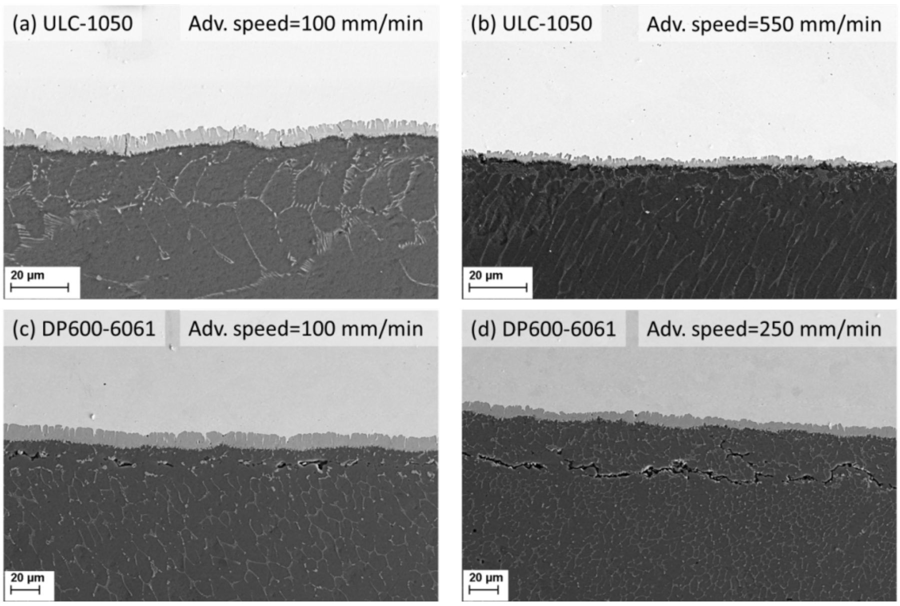

Figure 8: Development of solidification porosity in Al at different advancing speeds of the tool for 1050 ((a) and (b)) and 6061 ((c) and (d)) Al alloys. Even at higher advancing speeds, 1050 shows almost no porosity, opposite to 6061, where porosity was always present for the chosen advancing speeds.

Conclusion

Aluminium alloys (1050, 2024 and 6061) have been successfully welded to ULC and DP steels in lap-joint configuration by means of a new friction melt bonding process. The metallurgical joint is achieved by the formation of a continuous intermetallic layer composed of $FeAl_3$ and Fe_2Al_5. The total thickness of the IML depends on the process parameters and materials, obtaining a very fine grained microstructure around 2-3 µm.

The boundary conditions and nature of the base materials are relevant in the thermal processing and final microstructure. The thermomechanically affected zone of ULC steel shows grain refining while DP steel is partially re-austenitized and re-transformed to bainite upon cooling. The presence of defects identified as hot tearing is dependent on the thermal cycles and the alloy composition.

Although lap-shear tests did not fully load the IML, the fracture in the base materials showed that, even if brittle, the presence of the IML did not deteriorate the mechanical resistance of the weld. The presence of porosities at larger advancing speeds for Al 2024 welds was a key factor in the loss of mechanical properties.

ACKNOWLEDGEMENTS

The authors acknowledge financial support from the Interuniversity Attraction Poles Program from the Belgian state through the Belgian Policy agency; contract IAP7/21 “INTEMATE”. N. Jiménez Mena and C. van der Rest are funded by a FRIA grant from the National Funds for Scientific Research (FRS-FNRS). P.J.J. acknowledges the FRS-FNRS.

REFERENCES

[1] X. Cui, H. Zhang, S. Wang, L. Zhang, J, Ko, Materials and Design 32 (2011) 815–821.
[2] H. Dong, L. Yang, C. Dong, S. Kou, Mater. Sci. Eng. A 534 (2012) 424–435.
[3] R. Qiu, H. Shi, K, Zhang, Y. Tu, C. Iwawoto, S. Satonaka, Materials Characterization 61 (2010) 684 – 688.

[4] R. Qiu, C. Iwawoto, S. Satonaka, Materials Characterization 60 (2009) 156–159.
[5] Y. Abe, T. Kato, K, Mori, J. Mater. Process. Technol. 209 (2009) 3914 - 3922.
[6] X. He, I. Pearson, K. Young, J. Mater. Process. Technol. 199 (2008) 27-36.
[7] S. Bozzi, A.L. Helbert-Etterm T. Baudin, B. Criqui, J.G. Kerbiguet, Mater. Sci. Eng. A 527 (2010) 4505–4509.
[8] C.M. Chen, R. Kovacevic, Int. J. Mach. Tools Manuf. 44 (2004) 1205–1214.
[9] T. Tanaka, T. Morishige, T. Hirata, Script. Mater. 61 (2009) 756–759
[10] G. Sierra, P. Peyre, F. Deschaux-Beaume, D. Stuart, G. Fras, Mater. Sci. Eng. A 447 (2007) 197–208
[11] S. Meco, G. Pardal, S. Ganguly, R. M. Miranda, L. Quintino, S. Williams, Int J Adv Manuf Technol 67 (2013) 647–654
[12] J. Fan, C. Thomy, F. Vollertsen, Physics Procedia 12 (2011) 134–141
[13] C. van der Rest, A. Simar, P.J. Jacques, Method for welding at least two layers (patent), International Publication No. WO2013164294 (A1), International Publication Date: 7 November, 2013.
[14] C. van der Rest, P.J. Jacques, A. Simar Script. Mater. 77 (2014) 25-28
[15] N. Tang, Y.P. Li b, S. Kurosu, Y. Koizumi, H. Matsumoto, A. Chiba, Corrosion Science 60 (2012) 32–37
[16] D. Naoi, M. Kajihara, Mater. Sci. Eng. A 459 (2007) 375–382
[17] K. Dehghani, A. Chabok, Mater. Sci. Eng. A 528 (2011) 4325–4330
[18] P. Xue, B.L. Xiao, W.G. Wang, Q. Zhang, D. Wang, Q.Z. Wang, Z.Y. Ma, Mater. Sci. Eng. A 575 (2013) 30–34
[19] C. Jonckheere, B. de Meester, A. Denquin, A. Simar, J. Mater. Process. Technol. 213 (2013) 826–837
[20] D.G. Eskin, Suyitno, L. Katgerman, Prog. Mater. Sci. 49 (2004) 629–711